BIOCHEMISTRY
including biophysical chemistry & molecular biology
Article

Biochemistry **2009,** *48,* 6291–6298 6291
DOI: 10.1021/bi900524m

Redox Properties of the Prosthetic Groups of Na^+-Translocating NADH:Quinone Oxidoreductase. 1. Electron Paramagnetic Resonance Study of the Enzyme[†]

Alexander V. Bogachev,[‡] Leonid V. Kulik,[§] Dmitry A. Bloch,[∥] Yulia V. Bertsova,[‡] Maria S. Fadeeva,[‡] and Michael I. Verkhovsky*,[∥]

[‡]*Department of Molecular Energetics of Microorganisms, A. N. Belozersky Institute of Physico-Chemical Biology, Moscow State University, Moscow 119992, Russia,* [§]*Institute of Chemical Kinetics and Combustion, Russian Academy of Sciences, 630090 Novosibirsk, Russia, and* [∥]*Institute of Biotechnology, P.O. Box 65 (Viikinkaari 1), University of Helsinki, Helsinki 00014, Finland*

Received March 27, 2009; Revised Manuscript Received May 27, 2009

ABSTRACT: Redox properties of all EPR-detectable prosthetic groups of Na^+-translocating NADH:quinone oxidoreductase (Na^+-NQR) from *Vibrio harveyi* were studied at pH 7.5 using cryo-EPR spectroelectrochemistry. Titration shows five redox transitions. One with $E_m = -275$ mV belongs to the reduction of the [2Fe-2S] cluster, and the four others reflect redox transitions of flavin cofactors. Two transitions ($E_m^1 = -190$ mV and $E_m^2 = -275$ mV) originate from the formation of FMN anion radical, covalently bound to the NqrC subunit, and its subsequent reduction. The remaining two transitions arise from the two other flavin cofactors. A high potential ($E_m = -10$ mV) transition corresponds to the reduction of riboflavin neutral radical, which is stable at rather high redox potentials. An $E_m = -130$ mV transition reflects the formation of FMN anion radical from a flavin covalently bound to the NqrB subunit, which stays as a radical down to very low potentials. Taking into account the EPR-silent, two-electron transition of noncovalently bound FAD located in the NqrF subunit, there are four flavins in Na^+-NQR all together. Defined by dipole−dipole magnetic interaction measurements, the interspin distance between the $[2Fe\text{-}2S]^+$ cluster and the NqrB subunit-bound FMN anion radical is found to be 22.5 ± 1.5 Å, which means that for the functional electron transfer between these two centers another cofactor, most likely FMN bound to the NqrC subunit, should be located.

NADH:quinone oxidoreductases from marine bacteria of the genus *Vibrio* form a family of primary redox-driven Na^+ pumps that generate transmembrane electrochemical sodium potential (*1*−*3*).

The Na^+-translocating NADH:quinone oxidoreductase (Na^+-NQR)[1] consists of six subunits (NqrA-F) (*4*) that correspond to the six genes of the *nqr* operon (*5*, *6*). Subunit NqrF possesses binding motifs for NADH, FAD, and a [2Fe-2S] cluster (*5*, *7*, *8*). Besides, Na^+-NQR bears two covalently bound FMN residues that are attached by phosphoester bonds to threonine residues in subunits NqrB and NqrC, respectively (*9*−*11*). Recently, a noncovalently bound riboflavin was also reported in Na^+-NQR (*12*, *13*). However, there are no data on which subunit of Na^+-NQR riboflavin is bound to.

Thus, Na^+-NQR is thought to contain the following set of cofactors: one [2Fe-2S] cluster, one noncovalently bound FAD, two covalently bound FMN residues, and one noncovalently bound riboflavin. The flavin cofactors of Na^+-NQR form three distinct radicals at equilibrium conditions that are detectable by EPR: (i) oxidized Na^+-NQR contains a neutral radical (*14*−*16*) which most likely arises from the riboflavin (*13*); (ii) the fully reduced enzyme harbors an anionic flavin radical (*14*−*16*), which is presumably stabilized on the FMN residue of the NqrB subunit (*13*, *17*); (iii) as has been recently shown, Na^+-NQR under weakly reducing conditions contains a second anionic radical, which was assigned to the semiquinone of the FMN residue of the NqrC subunit (*17*).

During *in vivo* functioning Na^+-NQR oxidizes NADH and transfers two electrons to ubiquinone with production of ubiquinol. This redox reaction is coupled with a vectorial transfer of two sodium ions across the membrane, thus showing the Na^+/e^- ratio to be 1 (*3*, *18*):

$$NADH + H^+_{in} + Q + 2Na^+_{in} \rightarrow NAD^+ + QH_2 + 2Na^+_{out}$$

The mechanism of energy conversion between the redox transitions and the transmembrane translocation of sodium ions in Na^+-NQR is still unknown. Redox titration of all Na^+-NQR

[†]This work was supported by Biocentrum Helsinki (project number 7919028), the Sigrid Jusélius Foundation (project number 4700827), the Magnus Ehrnrooth Foundation, the Academy of Finland (project number 115108), and the Russian Foundation for Basic Research (project numbers 07-04-00619 and 09-03-00013) and by a grant of the President of the Russian Federation for scientific schools (project number HIII-551.2008.3).

*To whom correspondence should be addressed. Phone: +358 9 191 58005. Fax: +358 9 191 58001. E-mail: michael.verkhovsky@helsinki.fi.

[1]Abbreviations: CW, continuous wave; DDM, *n*-dodecyl-*β*-D-maltoside; E_h, ambient redox potential; E_m, midpoint redox potential; ESE, electron spin−echo; ESEEM, electron spin−echo envelope modulation; Fl, oxidized flavin; FlH_2, neutral form of reduced flavin; FlH^-, anionic form of reduced flavin; $FlH^\bullet$, neutral flavosemiquinone radical; $Fl^{\bullet-}$, flavosemiquinone anion radical; Na^+-NQR, Na^+-translocating NADH:quinone oxidoreductase; PCR, polymerase chain reaction; RIDME, relaxation-induced dipolar modulation enhancement; Rf, riboflavin; SHE, standard hydrogen electrode.

Published on Web 06/04/2009

prosthetic groups at varied concentrations of Na^+ and at different pH seems to be a necessary step in understanding the operating mechanism of this enzyme. It is noteworthy that this task is not simple, because, for example, the four Na^+-NQR flavins have the same chemical nature and their optical spectra are very similar. Besides, the oxidation (reduction) of a flavin can proceed either through one step (two-electron process) or through two sequential one-electron steps (*19*), which complicates the task even further.

Earlier we have defined the properties of some of the Na^+-NQR redox cofactors at pH 7.5 using optical spectroscopy (*20*). In the present work, in order to make a complete description of the thermodynamic properties of all the redox-active prosthetic groups of the enzyme, the titration of the Na^+-NQR EPR spectra has been performed. Magnetic dipole−dipole coupling measurements were also employed to study the distances between the cofactors. To define the protonation states of the cofactors and to verify the EPR data, optical spectroelectrochemical titrations at different pH values have also been carried out [accompanying paper (*21*)].

MATERIALS AND METHODS

Bacterial Strains. A *Vibrio harveyi* strain bearing on the chromosome the complete *nqr* operon with six-histidine-tagged *nqr*F gene under control of the *nqr* promoter was constructed. The 5′ part of the *V. harveyi apb*E gene was amplified from genomic DNA using PCR with *Taq* polymerase and primers Vh_*apb*E_dir 5′-GTTAATCCCCGCAAGTGATTGAATC and Vh_*apb*E_rev 5′-GCCAGCTCTTTAAAACCATCGTCC. The amplified fragment (~1.1 kbp) was cloned into pGEM-T vector resulting in the pG_ApbE1 plasmid. The 3′ part of the *V. harveyi nqr*F gene fused with the six-histidine tag was cut from the pLN52his-1 plasmid (*20*) by *Spe*I and *Dra*I digestion and inserted into pKNOCK vector (*22*) between *Spe*I and *Sma*I sites resulting in the pKnFhis plasmid.

The blunted *Sph*I−*Pst*I fragment of the pG_ApbE1 plasmid was cloned into the *Sfr*274I site of pKnFhis, and a plasmid (pKnFhisA5) bearing the six-histidine-tagged *nqr*F gene together with the unidirectionally transcribing 5′ part of the *apb*E gene was selected. The kanamycin-resistance cassette from pUC4K vector was inserted between the *nqr*F and *apb*E genes of the pKnFhisA5 plasmid into the *Pst*I site. The unidirectional orientation of the kanamycin-resistance cassette and the *nqr*F and *apb*E genes was checked, and the final plasmid (pKnFhisAKm) was used for replacement of the native chromosomal *nqr*F gene of *V. harveyi* with the six-histidine-tagged *nqr*F. To do this, the pKnFhisAKm plasmid was transferred into the *V. harveyi* R3 (Rf^R) strain (*23*) via conjugation using *Escherichia coli* SM10λpir as the donor, and a $Tc^S\,Km^R\,Rf^R$ phenotype clone (VHtag60) characteristic of a double-crossover introduced mutation was selected. Localization of the mutation in the *V. harveyi* chromosome was verified by PCR analysis.

Enzyme Purification. His-tagged Na^+-NQR was purified using affinity chromatography. Membranes from cells of *V. harveyi* VHtag60 were suspended in solution A (350 mM KCl, 5 mM imidazole, 20 mM Tris-HCl, pH 8.0), solubilized with 1.5% potassium deoxycholate, and centrifuged at 200000*g* for 60 min. The supernatant was loaded onto a Ni-NTA column equilibrated with solution A containing 0.2% potassium deoxycholate. The column was successively washed with solution A containing 0.2% potassium deoxycholate and 10 mM imidazole and with solution A containing 0.05% *n*-dodecyl-β-D-maltoside (DDM) and 20 mM imidazole. Na^+-NQR was then eluted from the column with solution A containing 0.05% DDM and 100 mM imidazole. The enzyme obtained was concentrated and frozen at −80 °C until use.

Redox Titration of EPR Spectra. EPR spectroelectrochemical redox titrations were accomplished using a titration system analogous to one used by Harder et al. (*24*, *25*) with some modifications. A quartz tube (o.d. 5 mm, i.d. 4 mm, length 170 mm) was attached to a quartz-to-glass graded seal and then to an all-glass electrochemical compartment. The electrochemical cell utilizes a typical three-electrode circuit with saturated Ag/AgCl reference electrode, Pt foil counter electrode, and gold (99.99%) grid working electrode. The setup permits convenient transfer of the sample between the electrochemical compartment and the EPR tube by a simple rotation of the cell; thus oxygen leakage that would disturb the ambient potential during sample transfer is avoided. The buffer (400 μL) was degassed by cycling with vacuum and He (99.9999%); then the trace of oxygen was quenched electrochemically by poising the potential at −400 mV vs SHE. Under gas flow, buffer was removed, and sample (400 μL) in anaerobic buffer was added to the cell with a 1 mL gastight syringe (Hamilton). The sample contained ~20 μM Na^+-NQR in the buffer consisting of 100 mM KCl, 25 mM NaCl, 11.5% (v/v) glycerol, 0.1% DDM, 50 mM HEPES-Tris, pH 7.5, and mediators (200 μM cobalt(III) sepulchrate, E_m = −350 mV, 400 μM pentaamminechlororuthenium, E_m = −130 mV, and 200 μM hexaammineruthenium, E_m = +50 mV). The sample was degassed by cycling with vacuum and He; then the trace of oxygen was quenched electrochemically by poising the potential at −400 mV. A PAR263A potentiostat (Princeton Applied Research) was employed to poise the potential at the desired equilibrium value. When equilibrium had been achieved, as the changes in the cell current became no longer significant and a desired potential value could be stably maintained, the cell was tipped to transfer the solution to the EPR tube; the solution was then transferred back to the electrochemical compartment, and the potential stability was checked. The sample was then transferred again to the EPR tube and immediately frozen in liquid nitrogen for EPR spectroscopy. This cycle was repeated to obtain a titration curve. Titrations were performed in both oxidative and reductive directions with no significant hysteresis detected. All redox potentials quoted refer to the SHE.

CW-EPR Spectroscopy. A Bruker ESP-300 X-band (9.4 GHz) EPR spectrometer was used. The field modulation frequency was 100 kHz. The temperature of the sample (80 K) was controlled with an ESR 900 liquid helium cryostat with an ITC4 temperature controller (Oxford Instruments). The frequency was calibrated with a HP X532B microwave frequency meter. The EPR signals were quantified by double integration of the experimental spectra obtained at nonsaturated conditions. All spectra were normalized for microwave power, modulation amplitude, and gain. The spectra were simulated using WinEPR SimFonia Version 1.26 (beta) software (Bruker Analytic GmbH).

Pulsed EPR Spectroscopy. Pulsed EPR experiments were performed using an Elexsys-580 FT EPR spectrometer equipped with a dielectric cavity (Bruker ER 4118 X-MD-5) inside an Oxford Instruments CF 935 cryostat, which was cooled by helium flow. The pulse sequences used were primary echo ($\pi/2-\tau-\pi-\tau-$echo), inversion−recovery ($\pi-T-\pi/2-\tau-\pi-\tau-$echo), and stimulated echo ($\pi/2-\tau-\pi/2-T-\pi/2-\tau-$echo). The durations of the $\pi/2$ and π microwave pulses were 8 and 16 ns,

respectively. The whole echo signal in time domain was integrated. The repetition time of the experiment was chosen to avoid substantial saturation of the echo signal. Typically, it was about 90% of the maximum (unsaturated) value. The temperature was 30 K.

Two Na^+-NQR samples were used for pulsed EPR experiments. In the first sample Na^+-NQR was poised at redox potential of −160 mV. To do this the protein (approximately at concentration of 200 μM) was anaerobically incubated in 50 μL of buffer (20 mM HEPES/Tris, pH 7.5, 100 mM NaCl, and 0.1% DDM) containing 0.4 mM L-lactate, 40 mM pyruvate, 5 mM NAD^+, and 1 Unit of lactate dehydrogenase. The second sample contained Na^+-NQR reduced by 10 mM sodium dithionite. The samples were prepared in quartz tubes of 4.8 mm outer diameter.

Protein content was determined by the bicinchoninic acid method using bovine serum albumin as a standard.

Sodium concentration was measured by flame photometry.

RESULTS AND DISCUSSION

CW-EPR Redox Titration. The isolated Na^+-NQR shows two types of EPR signals. One is the signal from the reduced [2Fe-2S] cluster ($g_{xy} = 1.94$, $g_z = 2.02$) (*14*, *26*), and the other is a radical signal with $g = 2.00$. The latter feature represents not a unique radical but rather a complex set of signals from different states of the flavin cofactors (*14*, *26*). In order to establish the nature of these radical signals, we performed a potentiometric redox titration of the EPR lines using the *V. harveyi* enzyme at pH 7.5. Figure 1 shows the development of the radical signal (A) and the $[2Fe\text{-}2S]^+$ cluster signal (B) as the redox potential changes from +130 to −430 mV. All presented data and further manipulation were done with spectra obtained under nonsaturating microwave power conditions, and the saturation was checked at each point of the titration (data not shown).

The redox titration profile for the $[2Fe\text{-}2S]^+$ cluster signal located around $g = 1.94$ is shown in Figure 2A (squares). In our previous work (*14*) the midpoint redox potential of the [2Fe-2S]

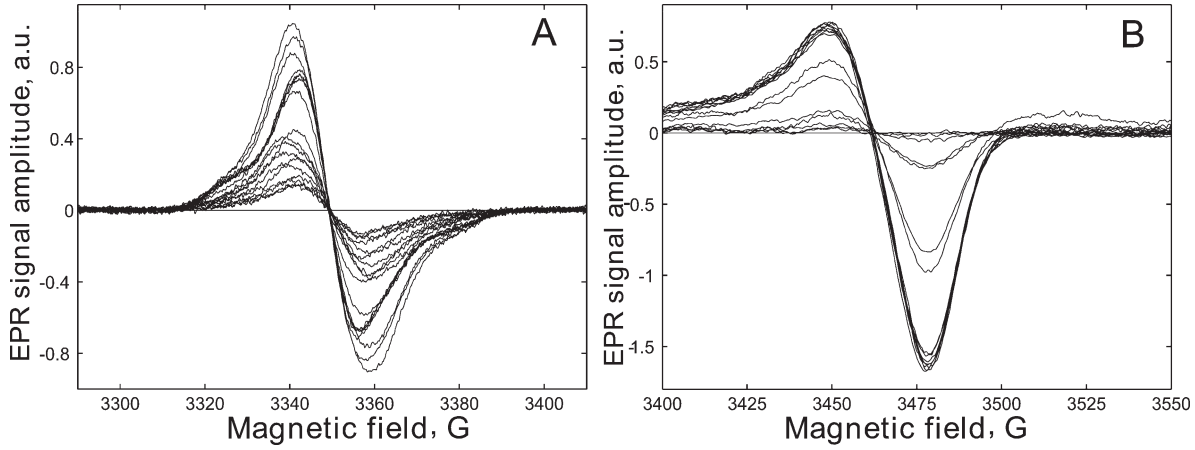

FIGURE 1: EPR spectra of the flavin radicals ($g = 2.00$) (A) and the [2Fe-2S] cluster ($g_{xy} = 1.94$) (B) at different ambient redox potentials. The redox potentials varied between −430 and +130 mV vs SHE. EPR conditions: microwave frequency, 9.385 GHz; temperature, 80 K; microwave power, 3.2 μW (A) or 10 mW (B); modulation amplitude, 0.67 mT (A) or 1.27 mT (B). At the chosen microwave powers neither components of the EPR spectra are saturated as found from the dependence of the EPR signals on microwave power. Conditions: enzyme concentration, 20 μM; KCl, 100 mM; NaCl, 25 mM; glycerol, 11.5% (v/v); DDM, 0.1%; HEPES/Tris (pH 7.5), 50 mM; and mediators (200 μM cobalt(III) sepulchrate, 400 μM pentaamminechlororuthenium, and 200 μM hexaammineruthenium).

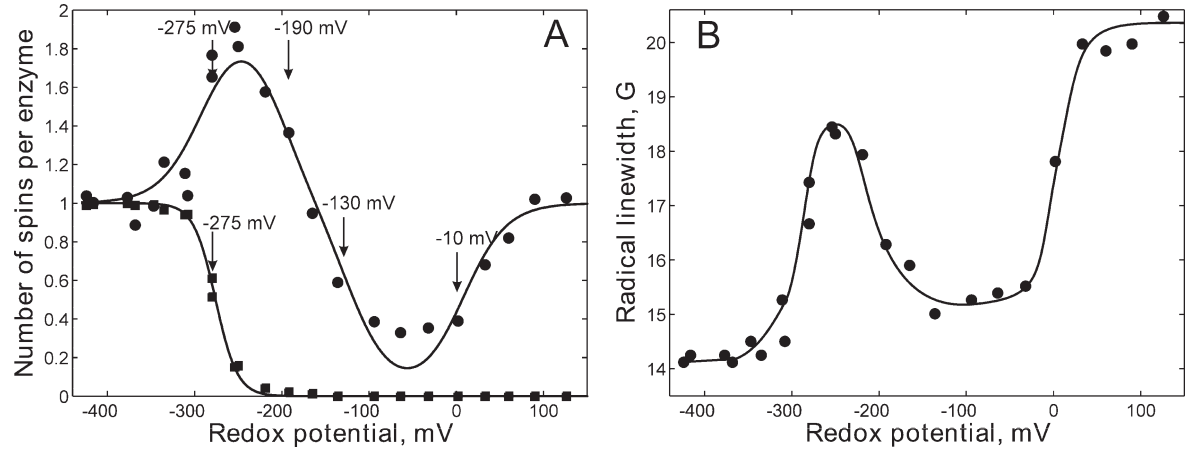

FIGURE 2: Redox titration of spin concentration (A) and radical spectra line width (B) in Na^+-NQR. In panel A, the spin concentrations of the [2Fe-2S] cluster (squares) and flavin radical (circles) are shown. The line drawn through the squares is a theoretical Nernstian curve for a two-electron redox component, $E_m = -275$ mV. The line drawn through the cycles is a theoretical line of the titration of the three-component system, where the first component has two transitions, $FlH^- \leftrightarrow Fl^{\bullet -}$ ($E_m = -275$ mV) and $Fl^{\bullet -} \leftrightarrow Fl$ ($E_m = -190$ mV), the second component has only one transition, $Fl^{\bullet -} \leftrightarrow Fl$ ($E_m = -130$ mV), and the last component also has one transition, $FlH^- \leftrightarrow FlH^{\bullet}$ ($E_m = -10$ mV). The values of the potentials are the best fit result by the sum of four Nernstian transitions to the experimental points. Values of midpoint potentials are marked by arrows. Conditions: as in Figure 1.

cluster was found to be −268 mV (n = 1), also established by EPR titration. Note that the earlier titration was performed by varying the NADH/NAD^+ ratio in the absence of other redox mediators. Since NADH is a pure two-electron donor, such titration could give unexpected cooperative effects of either two or no electron delivery to the enzyme. The data represented in Figure 2A were obtained by electrochemical redox titration in the presence of a set of one-electron mediators (see Materials and Methods). These data fit well to a Nernstian curve with E_m = −275 mV, which is in a good agreement with our previous results (*14*). The major difference between the present data and the earlier data is the slope of the titration curve: in the present titration the curve is rather sharp and corresponds well to a two-electron process (n = 2). The reason why the [2Fe-2S] cluster, a classical one-electron carrier, shows the n = 2 titration curve remains unknown. A possible explanation is positive cooperativity between the reduction of the [2Fe-2S] cluster and other cofactors of the enzyme. Further experiments are required to clarify the possibility of such interaction.

The EPR spectra of the flavin radicals and the [2Fe-2S] cluster are partially overlapping (*26*, *27*). In order to separate them and to quantify the number of the radicals per enzyme molecule, the following approach was applied. The number of [2Fe-2S] clusters in the fully reduced enzyme was taken as 1 mol of spin/mol of enzyme. The EPR spectrum of the reduced [2Fe-2S] cluster was simulated (see Materials and Methods) with the parameters g_{xyz} = 1.929, 1.937, 2.017 and line widths = 14, 20, 12 G, respectively (*26*). The resulting model spectrum was normalized to match the observed spectrum of the [2Fe-2S] cluster for each redox potential in the region around g = 1.94, where only this cofactor has a band. Then this spectrum of the cluster was subtracted from the spectrum of Na^+-NQR at each redox potential to obtain pure spectra of the radicals. Then the spectra were double integrated and normalized to the quantity of the [2Fe-2S] cluster in the fully reduced enzyme. As a result we obtained the redox titration of the number of radical spins per enzyme molecule.

The dependence of the spin concentration in radical signal on the ambient redox potential is shown in Figure 2A (circles). The fully reduced enzyme contains equimolar spin concentration in the radical line and in the $[2Fe\text{-}2S]^+$ cluster signal, which is in agreement with earlier data (*15*, *16*). The radical signal in the fully reduced enzyme had line width ∼14.5 G (Figure 2B), which is characteristic to the flavosemiquinone anion (*28*).

According to our earlier optical spectroelectrochemical data (*20*) there are two different flavin cofactors in Na^+-NQR that are each capable of only one-electron reduction: (i) from neutral flavosemiquinone to the fully reduced flavin (E_m ∼ +20 mV) and (ii) from the oxidized flavin to flavosemiquinone anion (E_m ∼ −150 mV). In this case the EPR spectra titration should show a constant quantity of the radical signal (1 mol/mol of enzyme) with line width of 14−15 G in the potential range from −430 to −200 mV; further oxidation from −200 to −50 mV should decrease the number of radicals down to zero, and further increasing of the potential from −50 to +130 mV should result in an increase of the radical signal up to 1 mol/mol of enzyme but with the wider line width of ∼20 G (*14*). As can be seen in Figure 2A, the behavior of the radical titration curve at potentials from −150 to+130 mV correlates with the prediction, but increasing the potential in the range from −350 to −250 mV results in an increase of the spin concentration from 1 to ∼1.8 spins per enzyme molecule. This increase of the spin concentration shows the appearance of an additional radical, which was not detected in our earlier experiments.

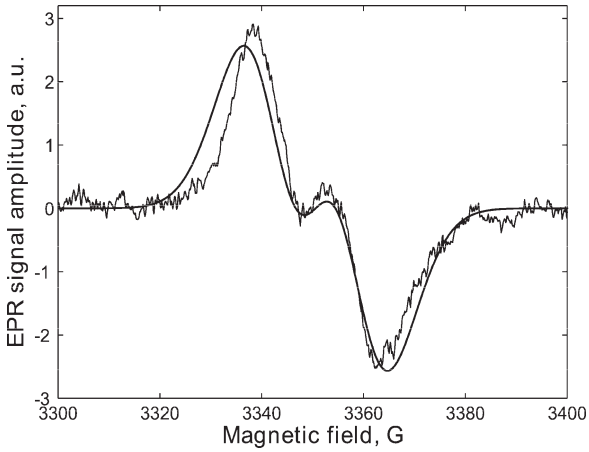

FIGURE 3: Difference EPR spectrum of the radical obtained by subtraction of the signal at −420 mV from the one at −250 mV. The experimental data (noisy curve) and a model curve (smooth line). The model spectrum was obtained by subtraction of the spectrum of one free electron equivalent with the line width of 14.5 G from the spectrum of two free electron equivalents with the line width of 18 G (see Results and Discussion for details). Conditions: as in Figure 1A.

Figure 2B shows that not only the amplitude but also the line width in the same range of potentials increases from 14.5 to 18 G. To determine the reason for such signal broadening, we analyzed the spectrum of the band appearing upon transition from −420 to −250 mV. This spectrum is shown in Figure 3. It has rather unusual shape characterized by an inflection in the g = 2.00 region and apparent line width of ∼24 G. Such complex spectral shape can hardly be attributed to the appearance of just an additional flavin radical signal. In the accompanying paper (*21*) where we analyzed the titration of optical spectra of Na^+-NQR, the changes in this region of the redox potentials revealed the appearance of the flavosemiquinone anion from the fully reduced flavin ($FlH^- \rightarrow Fl^{\bullet -}$), which, however, does not correlate well with the shape and the line width of the EPR spectrum presented in Figure 3.

From our point of view, the most plausible scenario of the appearance of the signal presented in Figure 3 should take into account the possibility of a dipole−dipole magnetic interaction between the two anionic radicals, one which was already present at very low potentials and the other one which appears upon increasing of the redox potential. If these flavosemiquinones are located close to each other, such interaction would result in the broadening of *both* radical absorption bands. Thus the "−250 mV minus −420 mV" spectrum can be described as the appearance of *two* broad radical signals and disappearance of *one* narrow (14.5 G) radical signal. To simulate this spectrum, we subtracted the spectrum of 1 equiv of free electron with the bandwidth 14.5 G from the spectrum of 2 equiv of free electron with the same larger line widths. The reasonable line shape (Figure 3, smooth line) was obtained at half-width of 18 G for the broad signals.

Figure 2A shows that the further oxidation of the protein in the range of potentials from −250 to −50 mV decreases the radical spin concentration down to ∼0.3 per Na^+-NQR complex. The decrease of spin concentration goes together with narrowing of its line width to ∼15 G (Figure 2B). This confirms that the disappearance of the second anion radical returns the line shape of the remaining one to the spectrum characteristic for the flavin anion radical.

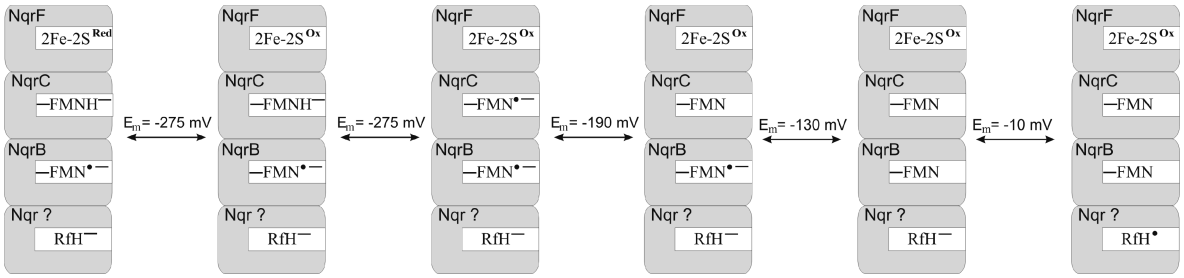

FIGURE 4: Scheme of EPR-detectable redox transitions in Na^+-NQR during electrochemical redox titration. The information on protonation state of the reduced cofactors was obtained from the pH dependence of their midpoint redox potentials (*21*).

The last transition seen in Figure 2A shows again increase of the radical spin concentration upon increasing the potential from −50 to +130 mV. This radical signal has line width of 20 G (Figure 2B), and its content at the high potential reaches 1 mol of spin/mol of the enzyme (Figure 2A). Such parameters are characteristic for the neutral flavosemiquinone well described earlier (*9*, *12*).

The redox titration of all EPR-detectable cofactors allowed us to determine the thermodynamic properties of the one [2Fe-2S] cluster and three flavin cofactors, which is summarized in Figure 4. According to the scheme three of the four flavins of the protein exist in the stable semiquinone form at particular ambient redox potentials. Two of them (most likely the FMN residue covalently bound to subunit NqrB and a noncovalently bound riboflavin (*13*, *17*)) are able to perform only one-electron transitions under physiological conditions. For the riboflavin it is the $RfH^{\bullet} \rightarrow RfH^{-}$ transition (*20*) with $E_m = -10$ mV, and for the FMN_{NqrB} residue it is the $FMN \rightarrow FMN^{\bullet -}$ transition with $E_m = -130$ mV. The third flavin cofactor (most likely the FMN residue covalently bound to subunit NqrC (*13*, *17*)) undergoes two sequential one-electron transitions, $FMNH^{-} \rightarrow FMN^{\bullet -}$ and $FMN^{\bullet -} \rightarrow FMN$, with E_m values of −275 and −190 mV, respectively, with the maximal population of semiquinone about 0.8 at pH 7.5 (the detailed explanation on how the particular redox transition was assigned to the particular prosthetic group is given in the accompanying paper (*21*)). The solid line in Figure 2A, which fits the data reasonably well, was obtained by application of the proposed model, and the values of the above-mentioned midpoint potentials were determined as the best parameters for the fit.

The scheme itself (Figure 4) and all obtained values of the midpoint potentials are in good agreement with the results which we obtained by the redox titration of the Na^+-NQR optical spectra (see accompanying paper (*21*)).

Effect of Sodium Ion Concentration on Midpoint Redox Potentials of Na^+-NQR Cofactors. To check how the thermodynamic property of the enzyme cofactors would depend on the sodium ion concentration, the EPR spectra were titrated in the absence of added Na^+ (residual Na^+ concentration was ≈40 μM). The results of this titration (data not shown) were the same as those described above, although the latter was obtained in the presence of 20 mM NaCl. The absence of dependency of midpoint potentials of EPR-detectable Na^+-NQR cofactors on sodium ion concentration shows that the reduction of neither of these cofactors is coupled to sodium binding under equilibrium conditions.

Determination of Distance between Prosthetic Groups of Na^+-NQR by Pulsed EPR. The fully reduced Na^+-NQR contains two paramagnetic centers: (i) $[2Fe\text{-}2S]^+$ cluster and (ii) flavosemiquinone anion form of an FMN residue bound to the NqrB subunit. At the same time the enzyme poised at redox potential of ≈−150 mV should contain almost only the latter (see Figure 2). Such arrangement lets us compare EPR properties of this radical coupled with either paramagnetic or diamagnetic [2Fe-2S] cluster and make an estimate of the distance between these two prosthetic groups.

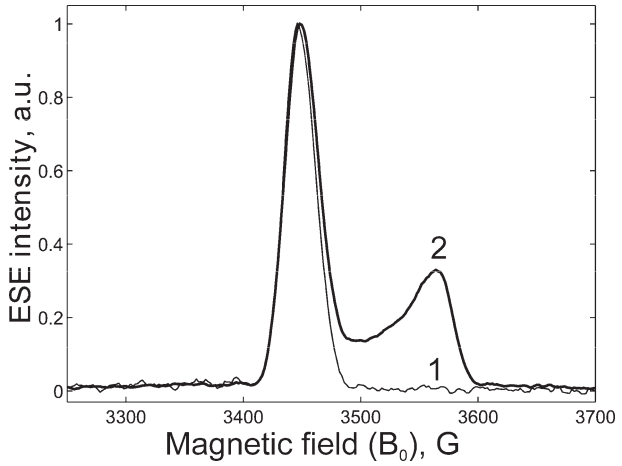

FIGURE 5: Two-pulse echo detected EPR spectra for Na^+-NQR poised at $E_h = -160$ mV (sample 1; thin line 1) and for Na^+-NQR reduced by excess of dithionite (sample 2; thick line 2). $\tau = 120$ ns; shot repetition time = 20 ms. Microwave frequency was 9.6757 GHz for sample 1 and 9.6754 GHz for sample 2. For other conditions, see Materials and Methods for details.

Two Na^+-NQR samples were used for this purpose. In the first sample (sample 1) the major paramagnetic species was the anionic semiquinone of FMN in the NqrB subunit (Na^+-NQR poised at $E_h = -160$ mV). In sample 2 (Na^+-NQR reduced by excess dithionite), this FMN radical was coupled to paramagnetic ($S = {}^1/_2$) [2Fe-2S] cluster. Figure 5 shows echo-detected EPR spectra of sample 1 (thin line 1) and sample 2 (thick line 2) measured in two-pulse sequence with $\tau = 120$ ns. The strong peak with the maximum near 3450 G, which is present in both spectra, corresponds to the EPR signal of anionic flavin radical. In sample 2 the EPR signal from [2Fe-2S] cluster is also present. The maximum of this signal is at 3565 G, and its low-field edge overlaps with the flavin radical signal.

Pulsed techniques can be applied for determination of the distance between two paramagnetic centers (*29*). It is important for the success of distance determinations that the values of spin−lattice (T_1) and spin−spin (T_2) relaxation times for the radical as well as for [2Fe-2S] cluster are not too short. The spin−spin relaxation times can be found through the analysis of primary echo decay traces (analysis of the echo amplitude as a function of pulse separation, τ). Line 2 in Figure 6 shows such trace for flavin radical in sample 1 ($B_0 = 3447$ G). Line 1 in this figure shows the

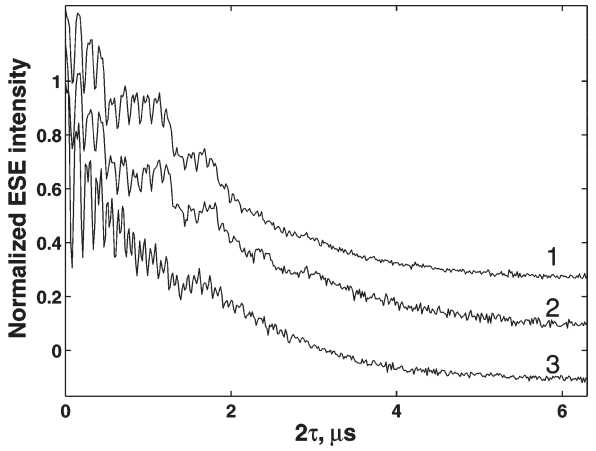

FIGURE 6: Two-pulse echo decay traces for flavin radical in sample 1 (B_0 = 3447 G, line 2), for flavin radical in sample 2 (B_0 = 3448G, line 1), and for [2Fe-2S] cluster in sample 2 (B_0 = 3565 G, line 3). The deviations at early time are due to electron spin−echo envelope modulation (ESEEM). Shot repetition time was 20 ms for flavin radical and 0.45 ms for [2Fe-2S] cluster. The curves for better representation were shifted from each other by 0.2. Conditions as for Figure 5.

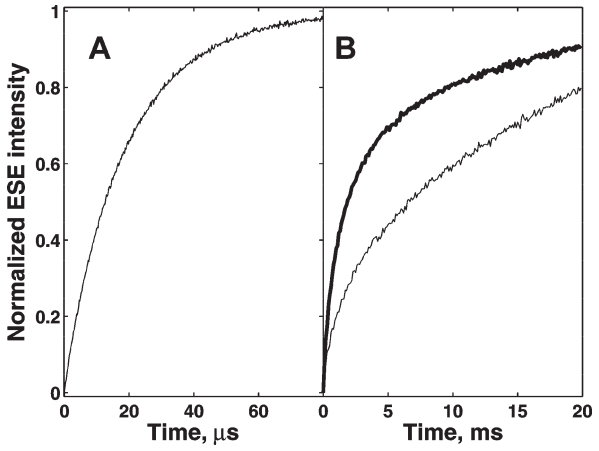

FIGURE 7: Inversion−recovery trace for (A) [2Fe-2S] cluster, B_0 = 3565 G, sample 2 (shot repetition time was 0.1 ms), and (B) flavin radical in sample 1 (thin line) and in sample 2 (thick line). τ = 120 ns, shot repetition time = 20 ms.

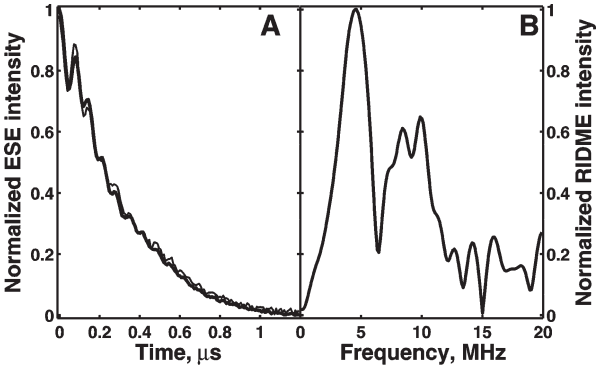

FIGURE 8: (A) RIDME time domain traces (stimulated echo decay trace with fixed T = 100 μs and scanned τ) for flavin radical in sample 1 (thin line) and for flavin radical in sample 2 (thick line). (B) Absolute value FT spectrum obtained from RIDME traces in (A). For the procedure of the FT spectrum calculation see Results and Discussion. Conditions: see Materials and Methods for details.

same decay for sample 2 (B_0 = 3448 G). Since it partly overlaps with the spectrum of the [2Fe-2S] cluster, a small contribution to its EPR signal is present in this trace. From the fitting of these decays to a monoexponential function the apparent transverse relaxation rates of the radical T_2 = 2.5 μs for sample 1 and T_2 = 2.2 μs for sample 2 were obtained. The pure echo decay trace for the [2Fe-2S] cluster (B_0 = 3565 G, sample 2) is shown in Figure 6 (line 3). This trace reveals the transverse relaxation rate of the [2Fe-2S] cluster, T_{2f} = 1.7 μs. Similar values of T_2 were found for other spectral positions corresponding to the [2Fe-2S] cluster EPR signal, which proves that T_{2f} is not orientation dependent.

For the determination of T_1 values inversion−recovery traces were measured. The thin line in Figure 7A shows the experimental trace for the [2Fe-2S] cluster (B_0 = 3565 G, sample 2). It is nicely approximated by a monoexponential function, from which the spin−lattice relaxation rate of the [2Fe-2S] cluster T_{1f} = 18.6 μs was obtained. Measurements at different spectral positions show that it is not orientation-dependent, similar to T_{2f}. The inversion−recovery traces for flavin radical in sample 1 (thin line) and sample 2 (thick line) can be seen in Figure 7B. The recovery is clearly not monoexponential. The curves can be satisfactorily simulated by a biexponential process, from which two characteristic times for each trace were obtained (1.2 and 18 ms for sample 1; 1.0 and 8.1 ms for sample 2), all of which are much larger than T_{1f} of the [2Fe-2S] cluster. Inspection of Figures 6 and 7 shows that both spin−spin and spin−lattice relaxation times of the flavin radical are smaller for sample 2 than those for sample 1. We suggest that the origin of this relaxation rate increase is the dipolar interaction of the spin of flavin radical with the fast-relaxing spin of the [2Fe-2S] cluster. This interaction lets us define the distance between the investigated paramagnetic centers performed by a RIDME experiment.

In the RIDME experiment the stimulated echo is measured with fixed T interval and scanned τ. The spin−lattice relaxation of the nonresonance electron spin located in the vicinity of the resonance spin shifts the frequency of its Larmor precession. This leads to the modulation of the stimulated echo intensity. The frequency of this modulation is determined by the strength of the dipolar interaction between the resonance and nonresonance spins, which in turn depends on the distance between these spins. The thick line in Figure 8A shows the stimulated echo decay trace with fixed T = 100 μs and scanned τ (RIDME experiment) for sample 2, B_0 = 3448 G. For such long T interval the contribution of the [2Fe-2S] cluster to stimulated echo intensity decays completely. However, since flavin radical has much longer spin−lattice relaxation time, its ESE signal is still present. Sample 1 was used as a "reference" in the RIDME experiment. The trace obtained for sample 1 in the same RIDME experiment is shown as the thin line in Figure 8A. There was some difference between the traces in Figure 8A, which is attributed to the RIDME effect caused by the longitudinal relaxation of the [2Fe-2S] spin in sample 2. Also, modulations with frequency of about 15 MHz are present in both traces, which is the usual proton ESEEM.

To separate the RIDME contribution to the modulation pattern from nuclear ESEEM and stimulated echo decay, the following approach was applied (similar to that done in refs (*29*) and (*30*)). We suppose that the stimulated echo intensity in sample 2 $S_2(\tau)$ can be factorized as

$$S_2(\tau) = r(\tau)n(\tau)d(\tau)$$

where $r(\tau)$ is the dipolar modulation caused by the RIDME effect, $n(\tau)$ is the nuclear ESEEM, and $d(\tau)$ is the function which describes the stimulated echo decay due to spin−spin relaxation.

For sample 1 the dipolar modulation is absent, so the stimulated echo intensity is

$$S_1(\tau) = n(\tau)d(\tau)$$

Thus, the dipolar modulation part can be obtained as a ratio:

$$r(\tau) = \frac{S_2(\tau)}{S_1(\tau)}$$

According to this approach the following procedure was done. First, the ratio $r(\tau) = S_2(\tau)/S_1(\tau)$ of the two traces in Figure 8A was obtained. The nonmodulated part of this ratio was approximated by a second-order polynomial and then subtracted. The result was multiplied by the Gaussian apodization function $G(\tau) = (a\tau)^2$ with the apodization factor $a = 1$ MHz. After that zero filling to 1024 points and Fourier transformation were performed. The resulting absolute value FT spectrum is presented in Figure 8B. Note that the intensity of the spectrum in the region around the proton Zeeman frequency $\nu_H \approx 15$ MHz is close to zero, which proves that proton ESEEM is efficiently suppressed by the applied procedure.

As can be seen, the main peak is at 4.5 ± 1 MHz. The intensity of this peak increased with T increase in the RIDME experiment (data not shown), which is typical for the RIDME effect. Assuming that the peak at 4.5 MHz corresponds to the Pake spectrum singularity $f_\perp$, we can use the relation:

$$f_\perp = \frac{g_1 g_2 \beta^2}{r^3}$$

where g_1 and g_2 are g-factors of the flavin radical and [2Fe-2S] cluster, β is the Bohr magneton, and r is the distance between the spins in point−dipole approximation. Using the isotropic g-value $g_2 = 1.965$ for the [2Fe-2S] cluster and $g_1 = 2.00$ for the anionic flavin radical, we obtain $r = 22.5 \pm 1.5$ Å.

Thus, the $[2Fe\text{-}2S]^+ - FMN^{\bullet-}_{NqrB}$ interspin distance obtained for Na^+-NQR is 22.5 ± 1.5 Å. The point−dipole value of r is an "effective" distance between the average positions of the delocalized spin densities on the semiquinone and on the iron−sulfur cluster. To relate this value to the edge to edge distance between these centers, it is necessary to consider the spin density distributions. The center of gravity of the electron spin density of flavin radicals is localized near nitrogen atom at N(5) position of the central pyrazine ring, i.e., near the centrum of the isoalloxazine moiety (*31*, *32*). This is also the case for the $FMN^{\bullet-}_{NqrB}$ of Na^+-NQR, as was determined by ENDOR (electron−nuclear double resonance) experiments (*33*). The spin on the anionic semiquinone can be approximated as a point−dipole located at the barycenter of its spin density, which is ≤3.6 Å from the edges of the isoalloxazine ring. Thus, the $[2Fe\text{-}2S]^+ - FMN^{\bullet-}_{NqrB}$ edge to edge distance (r_e) should be $18.9 \text{ Å} \leq r_e \leq 22.5$ Å.

Electron transfer theory predicts (*34*) that at such distance the rate would be rather slow ($1-100\ s^{-1}$) to ensure the enzyme turnover number of $300\ s^{-1}$ (*16*). Thus the determined distance seems too large for the direct electron transport during the turnover time, and additional redox group(s) (probably the FMN residue bound to the NqrC subunit) should be located between the [2Fe-2S] cluster and the FMN from the NqrB subunit in the electron transport pathway within Na^+-NQR.

ACKNOWLEDGMENT

We are indebted to Prof. S. A. Dzuba for helpful discussions.

REFERENCES

1. Tokuda, H., and Unemoto, T. (1981) A respiration-dependent primary sodium extrusion system functioning at alkaline pH in the marine bacterium *Vibrio alginolyticus*. *Biochem. Biophys. Res. Commun. 102*, 265–271.
2. Tokuda, H., and Unemoto, T. (1982) Characterization of the respiration-dependent Na^+ pump in the marine bacterium *Vibrio alginolyticus*. *J. Biol. Chem. 257*, 10007–10014.
3. Bogachev, A. V., and Verkhovsky, M. I. (2005) Na^+-translocating NADH:quinone oxidoreductase: progress achieved and prospects of investigations. *Biochemistry (Moscow) 70*, 143–149.
4. Nakayama, Y., Hayashi, M., and Unemoto, T. (1998) Identification of six subunits constituting Na^+-translocating NADH-quinone reductase from the marine *Vibrio alginolyticus*. *FEBS Lett. 422*, 240–242.
5. Rich, P. R., Meunier, B., and Ward, F. B. (1995) Predicted structure and possible ionmotive mechanism of the sodium-linked NADH-ubiquinone oxidoreductase of *Vibrio alginolyticus*. *FEBS Lett. 375*, 5–10.
6. Hayashi, M., Hirai, K., and Unemoto, T. (1995) Sequencing and the alignment of structural genes in the *nqr* operon encoding the Na^+-translocating NADH-quinone reductase from *Vibrio alginolyticus*. *FEBS Lett. 363*, 75–77.
7. Turk, K., Puhar, A., Neese, F., Bill, E., Fritz, G., and Steuber, J. (2004) NADH oxidation by the Na^+-translocating NADH:quinone oxidoreductase from *Vibrio cholerae*: functional role of the NqrF subunit. *J. Biol. Chem. 279*, 21349–21355.
8. Barquera, B., Nilges, M. J., Morgan, J. E., Ramirez-Silva, L., Zhou, W., and Gennis, R. B. (2004) Mutagenesis study of the 2Fe-2S center and the FAD binding site of the Na^+-translocating NADH:ubiquinone oxidoreductase from *Vibrio cholerae*. *Biochemistry 43*, 12322–12330.
9. Zhou, W., Bertsova, Y. V., Feng, B., Tsatsos, P., Verkhovskaya, M. L., Gennis, R. B., Bogachev, A. V., and Barquera, B. (1999) Sequencing and preliminary characterization of the Na^+-translocating NADH:ubiquinone oxidoreductase from *Vibrio harveyi*. *Biochemistry 38*, 16246–16252.
10. Nakayama, Y., Yasui, M., Sugahara, K., Hayashi, M., and Unemoto, T. (2000) Covalently bound flavin in the NqrB and NqrC subunits of Na^+-translocating NADH-quinone reductase from *Vibrio alginolyticus*. *FEBS Lett. 474*, 165–168.
11. Hayashi, M., Nakayama, Y., Yasui, M., Maeda, M., Furuishi, K., and Unemoto, T. (2001) FMN is covalently attached to a threonine residue in the NqrB and NqrC subunits of Na^+-translocating NADH-quinone reductase from *Vibrio alginolyticus*. *FEBS Lett. 488*, 5–8.
12. Barquera, B., Zhou, W., Morgan, J. E., and Gennis, R. B. (2002) Riboflavin is a component of the Na^+-pumping NADH-quinone oxidoreductase from *Vibrio cholerae*. *Proc. Natl. Acad. Sci. U.S.A. 99*, 10322–10324.
13. Juárez, O., Nilges, M. J., Gillespie, P., Cotton, J., and Barquera, B. (2008) Riboflavin is an active redox cofactor in the Na^+-pumping NADH:quinone oxidoreductase (Na^+-NQR) from *Vibrio cholerae*. *J. Biol. Chem. 283*, 33162–33167.
14. Bogachev, A. V., Bertsova, Y. V., Barquera, B., and Verkhovsky, M. I. (2001) Sodium-dependent steps in the redox reactions of the Na^+-motive NADH:quinone oxidoreductase from *Vibrio harveyi*. *Biochemistry 40*, 7318–7323.
15. Bogachev, A. V., Bertsova, Y. V., Ruuge, E. K., Wikström, M., and Verkhovsky, M. I. (2002) Kinetics of the spectral changes during reduction of the Na^+-motive NADH:quinone oxidoreductase from *Vibrio harveyi*. *Biochim. Biophys. Acta 1556*, 113–120.
16. Barquera, B., Hellwig, P., Zhou, W., Morgan, J. E., Hase, C. C., Gosink, K. K., Nilges, M., Bruesehoff, P. J., Roth, A., Lancaster, C. R., and Gennis, R. B. (2002) Purification and characterization of the recombinant Na^+-translocating NADH:quinone oxidoreductase from *Vibrio cholerae*. *Biochemistry 41*, 3781–3789.
17. Barquera, B., Ramirez-Silva, L., Morgan, J. E., and Nilges, M. J. (2006) A new flavin radical signal in the Na^+-pumping NADH:quinone oxidoreductase from *Vibrio cholerae*. An EPR/electron nuclear double resonance investigation of the role of the covalently bound flavins in subunits B and C. *J. Biol. Chem. 281*, 36482–36491.
18. Bogachev, A. V., Murtazina, R. A., and Skulachev, V. P. (1997) The Na^+/e^- stoichiometry of the Na^+-motive NADH:quinone oxidoreductase in *Vibrio alginolyticus*. *FEBS Lett. 409*, 475–477.
19. Massey, V. (2000) The chemical and biological versatility of riboflavin. *Biochem. Soc. Trans. 28*, 283–296.
20. Bogachev, A. V., Bertsova, Y. V., Bloch, D. A., and Verkhovsky, M. I. (2006) Thermodynamic properties of the redox centers of Na^+-translocating NADH:quinone oxidoreductase. *Biochemistry 45*, 3421–3428.

21. Bogachev, A. V., Bloch, D. A., Bertsova, Y. V., and Verkhovsky, M. I. (2009) Redox properties of the prosthetic groups of Na^+-translocating NADH:quinone oxidoreductase. 2. Study of the enzyme by optical spectroscopy, *Biochemistry* (DOI 10.1021/bi900525v).
22. Alexeyev, M. F. (1999) The pKNOCK series of broad-host-range mobilizable suicide vectors for gene knockout and targeted DNA insertion into the chromosome of gram-negative bacteria. *BioTechniques 26*, 824–826, 828.
23. Fadeeva, M. S., Yakovtseva, E. A., Belevich, G. A., Bertsova, Y. V., and Bogachev, A. V. (2007) Regulation of expression of Na^+-translocating NADH:quinone oxidoreductase genes in *Vibrio harveyi* and *Klebsiella pneumoniae*. *Arch. Microbiol. 188*, 341–348.
24. Harder, S. R., Lu, W. P., Feinberg, B. A., and Ragsdale, S. W. (1989) Spectroelectrochemical studies of the corrinoid/iron-sulfur protein involved in acetyl coenzyme A synthesis by *Clostridium thermoaceticum*. *Biochemistry 28*, 9080–9087.
25. Harder, S. R., Feinberg, B. A., and Ragsdale, S. W. (1989) A spectroelectrochemical cell designed for low temperature electron paramagnetic resonance titration of oxygen-sensitive proteins. *Anal. Biochem. 181*, 283–287.
26. Pfenninger-Li, X. D., Albracht, S. P., van Belzen, R., and Dimroth, P. (1996) NADH:ubiquinone oxidoreductase of *Vibrio alginolyticus*: purification, properties, and reconstitution of the Na^+ pump. *Biochemistry 35*, 6233–6242.
27. Fadeeva, M. S., Bertsova, Y. V., Verkhovsky, M. I., and Bogachev, A. V. (2008) Site-directed mutagenesis of conserved cysteine residues in NqrD and NqrE subunits of Na^+-translocating NADH:quinone oxidoreductase. *Biochemistry (Moscow) 73*, 123–129.
28. Palmer, G., Muller, F., and Massey, V. (1971) Electron paramagnetic resonance studies on flavoprotein radicals, in Flavins and Flavoproteins (Kamin, H., Ed.) pp 123−139, University Park Press, Baltimore, MD.
29. Kulik, L. V., Dzuba, S. A., Grigoryev, I. A., and Tsvetkov, Y. D. (2001) Electron dipole-dipole interaction in ESEEM of nitroxide biradicals. *Chem. Phys. Lett. 343*, 315–324.
30. Kulik, L. V., Grishin, Y. A., Dzuba, S. A., Grigoryev, I. A., Klyatskaya, S. V., Vasilevsky, S. F., and Tsvetkov, Y. D. (2002) Electron dipole-dipole ESEEM in field-step ELDOR of nitroxide biradicals. *J. Magn. Reson. 157*, 61–68.
31. Kay, C. W. M., Elsasser, C., Bittl, R., Farrell, S. R., and Thorpe, C. (2006) Determination of the distance between the two neutral flavin radicals in augmenter of liver regeneration by pulsed ELDOR. *J. Am. Chem. Soc. 128*, 76–77.
32. Fielding, A. J., Usselman, R. J., Watmough, N., Slinkovic, M., Frerman, F. E., Eaton, G. R., and Eaton, S. S. (2008) Electron spin relaxation enhancement measurements of interspin distances in human, porcine, and *Rhodobacter* electron transfer flavoprotein-ubiquinone oxidoreductase (ETF-QO). *J. Magn. Reson. 190*, 222–232.
33. Barquera, B., Morgan, J. E., Lukoyanov, D., Scholes, C. P., Gennis, R. B., and Nilges, M. J. (2003) X- and W-band EPR and Q-band ENDOR studies of the flavin radical in the Na^+ -translocating NADH:quinone oxidoreductase from *Vibrio cholerae*. *J. Am. Chem. Soc. 125*, 265–275.
34. Page, C. C., Moser, C. C., Chen, X., and Dutton, P. L. (1999) Natural engineering principles of electron tunnelling in biological oxidation-reduction. *Nature 402*, 47–52.